

Spectroscopic signature of magnetic bistability in Mn_2O^- anions and its implications for piezomagnetism at the nanoscale

S. N. Khanna and P. Jena

Department of Physics, Virginia Commonwealth University, Richmond, Virginia 23284-2000 USA

W.-J. Zheng, J. M. Nilles, and K. H. Bowen

Department of Chemistry, Johns Hopkins University, Baltimore, Maryland 21218 USA

(Received 15 December 2003; published 19 April 2004)

A synergistic study, using gradient corrected density functional theory and photoelectron spectroscopy, shows that the presence of oxygen can fundamentally alter the interaction between two Mn atoms. The normally weak interaction between two Mn atoms exhibits strong bonding when an oxygen atom is added to form Mn_2O . This allows the atomiclike magnetic moments of each Mn atom to couple either ferromagnetically or antiferromagnetically depending on whether Mn_2O is anionic or neutral. Furthermore, the Mn_2O^- anion is found to possess an antiferromagnetic isomer that lies only 0.01 eV above its nearly degenerate ferromagnetic ground state. The possibility of exploiting this magnetic bistability in the design of nanoscale piezomagnetic materials is discussed.

DOI: 10.1103/PhysRevB.69.144418

PACS number(s): 75.75.+a, 78.67.Bf, 79.60.Jv

I. INTRODUCTION

The manganese atom has a unique electronic structure. Its valence manifold is characterized by $3d^5 4s^2$ shells which are separated by a large energy gap of 8.4 eV. Because of its filled $4s$ shell, a Mn atom interacts weakly with another Mn atom. Consequently, the Mn_2 dimer forms a van der Waals complex that has the smallest binding energy and longest bond length of any dimer in the $3d$ -transition metal series.¹ Similarly, the cohesive energy of bulk Mn is also the lowest among the $3d$ -metals.²

The half-filled $3d$ -shell of the Mn atom empowers it to carry a magnetic moment of $5\mu_B$ each. As Mn atoms coalesce to form clusters or crystals, the large energy gap between the half filled $3d$ and filled $4s$ shell prevents significant overlap between these orbitals and thus Mn atoms continue to carry a magnetic moment of $5\mu_B$ each, irrespective of their environment. Nevertheless, the coupling between these moments can range from antiferromagnetic to ferrimagnetic to ferromagnetic. For example, a Mn_2 dimer isolated in a rare gas matrix,¹ is antiferromagnetic as is the Mn crystal, but small Mn clusters consisting of 3–5 atoms are ferromagnetic.^{3–6}

Using a synergistic approach involving first principles calculation and photodetachment spectroscopy, we show that an oxygen atom, mediating the coupling between Mn atoms, has a major effect on their binding energy and magnetic coupling. The binding energy of Mn_2O is very large, namely, 7.78 eV compared to 0.1 ± 0.1 binding energy of the Mn_2 dimer. This arises from the strong covalent bonding between Mn and O atoms. In addition, our calculations show that the ground state of neutral Mn_2O is antiferromagnetic, whereas its ferromagnetic state, with a magnetic moment of $10\mu_B$, lies 0.17 eV above the antiferromagnetic ground state. The situation was found to reverse when an electron is attached. The ground state of Mn_2O^- becomes ferromagnetic with a magnetic moment of $11\mu_B$, but its antiferromagnetic configuration with a moment of $1\mu_B$ lies only 0.01 eV above the

ferromagnetic anion ground state. The near degeneracy of the two different magnetic configurations of the Mn_2O^- is supported by comparing our calculated photodetachment peaks with experiment. We also find that it is possible to change the magnetic configuration of Mn_2O^- from ferro to antiferro by only slightly changing its geometry, namely the Mn–O bond length and Mn–O–Mn bond angle. The ability to alter the magnetic coupling by small changes in the geometry or by addition of an electron may be exploited in the design and synthesis of piezomagnetic materials.

In Sec. II, we give the details of the calculation and the experimental procedure for measuring the negative ion photodetachment spectra. Section III presents the results and Sec. IV contains the conclusions.

II. DETAILS OF CALCULATIONS AND EXPERIMENTS

We now discuss our theoretical and experimental procedures. The calculations were carried out using the linear combination of atomic orbitals-molecular orbital (LCAO-MO) approach. The atomic orbitals were represented by an all-electron Gaussian basis. The total energies were calculated using density functional theory⁷ and the generalized gradient approximation for exchange-correlation potential.⁸ The geometries of neutral and anionic Mn_2O were optimized for all possible spin structures. For each spin multiplicity, $M = 2S + 1$, we computed the atomic forces at the Mn and O sites which were relaxed until the forces vanished. The threshold for zero force was set at 10^{-3} a.u./Bohr. The computations were carried out using the NRLMOL set of codes developed by Pederson and co-workers.^{9,10} For Mn we used 20 optimized Gaussians to construct a $7s$, $5p$, $4d$ basis set. For O a basis set of $5s$, $4p$, and $3d$ was constructed from 13 optimized Gaussians. For details about the optimization of the Gaussians, the reader is referred to Ref. 11.

Anion photoelectron spectroscopy is conducted by crossing a mass-selected beam of negative ions with a fixed frequency photon beam and energy-analyzing the resultant photodetached electrons.¹² In the apparatus used to perform

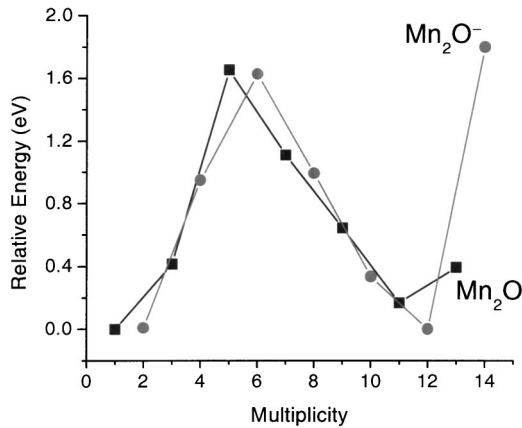


FIG. 1. The energy of neutral and anionic Mn_2O cluster as a function of spin multiplicity measured with respect to the lowest energy configuration.

these experiments, mass-selection was provided by time-of-flight mass spectrometry, photons for photodetachment were supplied by the third harmonic (3.49 eV) of a Nd:YAG laser, and electron energy analysis was provided by a magnetic bottle electron energy analyzer. Beams of Mn_nO^- , $n = 2-8$, were generated by laser ablating a rotating, translating manganese rod while pulsing oxygen doped helium over it.

III. RESULTS AND DISCUSSION

We first discuss our theoretical results. In Fig. 1 we plot the energies of both neutral Mn_2O and anionic Mn_2O^- for various spin multiplicities, M relative to the ground state. For each spin multiplicity, the two Mn atoms are treated as inequivalent, thus enabling them the freedom to carry different magnetic moments and spin orientations. The energies of neutral Mn_2O are measured with respect to the ground state, which is antiferromagnetic and thus has a total spin, S of 0, and hence $M=1$. The ferromagnetic isomer with the spin multiplicity $M=11$ (total magnetic moment of $10 \mu_B$) lies 0.17 eV above the antiferromagnetic state ($M=1$). Note that the configurations with intermediate spin multiplicities lie much higher in energy. The magnetic moment of each of the Mn atoms in the ferro- and antiferromagnetic configurations is nearly $5 \mu_B$.

In Fig. 1 we also plot the total energies of the anionic Mn_2O^- cluster for different spin multiplicities, $M' = 2S' + 1$. Once again the energies are measured with respect to the ground state configuration which now happens to be ferromagnetic with a spin multiplicity of $M=12$ (total moment of $11 \mu_B$). Here each Mn atom carries a moment of $5 \mu_B$ and O carries a moment of $1 \mu_B$. The antiferromagnetic state ($M=2$) is only 0.01 eV above the ferromagnetic state. Within the accuracy of our calculation, this energy difference is negligible, and hence both the configurations should coexist in the anion cluster beam. We will see from the experimental photodetachment spectra that this, indeed, is the case.

The geometries of the two low lying isomers of the neutral cluster are shown in Fig. 2. The Mn–O bond length and

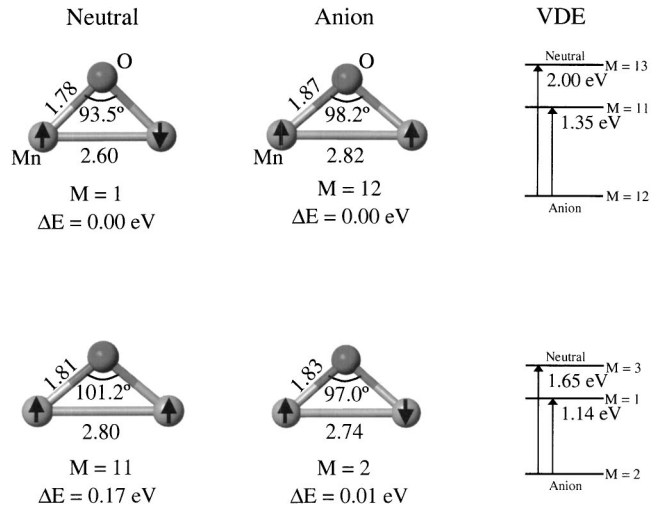


FIG. 2. The equilibrium geometries of neutral and anionic Mn_2O cluster isomers for ferromagnetic and antiferromagnetic configurations.

Mn–O–Mn bond angle in the ground state structure are, respectively, 1.78 Å and 93.5° , while they are 1.81 Å and 101.2° in its low energy isomer. The corresponding distance and bond angle in bulk manganese oxide are, respectively, 2.25 Å and 180° . Note that the Mn–Mn distance in the antiferromagnetic and ferromagnetic configurations are 2.60 Å and 2.80 Å, respectively. The near degeneracy in these configurations arises as Coulomb and exchange terms compete. While energy is gained from the exchange interaction in the ferromagnetic case, the shorter distance in the antiferromagnetic configuration benefits from the Coulomb contribution. In Fig. 2 we also plot the geometries of the two degenerate anion isomers. Note that the Mn–O and Mn–Mn distances are slightly enlarged compared to those in the neutral geometry having similar magnetic coupling. The Mn–O–Mn bond angles in the two isomers, on the other hand, are much closer than they are in the neutral isomers.

To establish the accuracy of our calculations, we compare our calculated results with experiment. In Fig. 3 we plot the photodetachment spectrum of the Mn_2O^- cluster. Note that there are three distinct peaks at binding energies of 1.56 eV, 1.75 eV, and 2.04 eV. These peaks arise from the vertical transitions from the anion ground state to the electronically excited states of the neutral having the same geometry as the anion. As the excess electron of the anion is photodetached, the resulting neutral cluster can exist in a spin multiplicity state, $M=M' \pm 1$, where M' is the ground state spin multiplicity of the anion. Consider the ground state of the anion first. Its spin multiplicity is $M'=12$. Thus the neutral following the electron ejection can have a spin multiplicity of $M=M'+1$ or $M'-1$, namely, $M=13$ or 11. Similarly, the spin multiplicity of the neutral originating from the nearly degenerate antiferromagnetic ($M'=2$) isomer of Mn_2O^- can be either 3 or 1. We have calculated these four transition energies by calculating the total energy of neutral Mn_2O cluster at the corresponding ground state geometry of the anion for the four different spin multiplicities discussed in the above. We show these transitions in Fig. 2. These vertical detach-

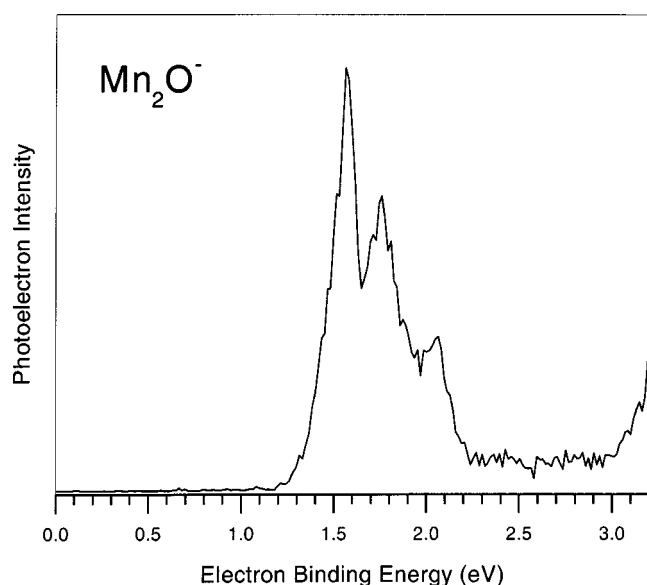


FIG. 3. The experimental photoelectron spectrum of the Mn_2O^- anion.

ment energies (VDE) from the ferromagnetic ground state of the anion lie at 1.14 eV, and 1.65 eV, while those from the antiferromagnetic anion isomer lie at 1.35 eV and 2.00 eV. Three of these peaks agree well with the experimental peaks at 1.56 eV, 1.75 eV, and 2.04 eV in Fig. 3. Based on our theoretically calculated transitions, the 2.04 eV peak in the experiment can only be explained if the transition occurs from the ferromagnetic state, while the 1.75 eV peak can only be explained if the transition occurs from the antiferromagnetic state. Thus, the agreement between theory and experiment provides confirmation that the anion has two nearly degenerate isomers with very different magnetic character. The only remaining issue is the absence of a peak in the experiment at 1.14 eV. Since the calculated VDE values tend to underestimate the actual VDE's by about 0.2 eV, moving the lowest predicted VDE up in energy would place it under the broad peak profile. Thus, the transition peak at 1.14 eV could be buried under the edge of the first peak in Fig. 3 which is broad. It is also possible that the transition probability corresponding to this transition is small. We have made no attempts to calculate this probability.

An alternate approach to analyze the negative ion photo-detachment spectra has recently been used by some authors.¹³ It is suggested that the spectra reflects the one electron levels in the negative ion and hence should be compared with density of electronic states in the anion. Since, such a comparison does not involve the neutral species, it cannot provide absolute positions of the energy peaks. It is then customary to shift the density of states of the anion so that the first peak in the density of states coincides with the experimental peak. The remainder of the density of states are then compared with the peaks beyond the first peak. In the present case, the ground state is marked by two isomers. We have therefore calculated the density of states in the two anion structures. To obtain a smooth density of states, we used a Gaussian broadening where a Gaussian of half width 0.14 eV was placed at each of the occupied levels. Further,

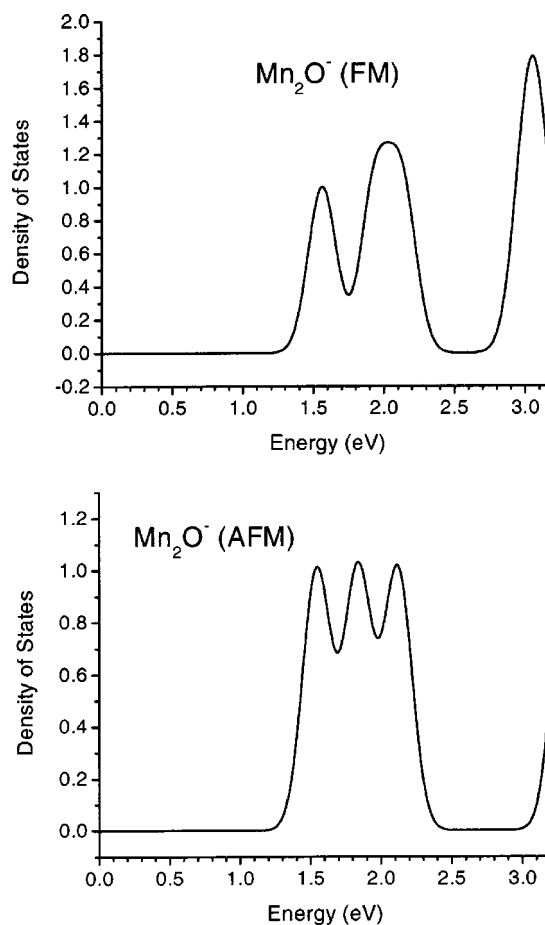


FIG. 4. The calculated density of states for the ferromagnetic and antiferromagnetic configuration of Mn_2O^- .

for each isomer, the position of the first peak in the density of states was adjusted to reproduce the first peak in photodetachment spectra of the anion.

Figure 4 shows the calculated density of states for the ferromagnetic and the antiferromagnetic anion. Note that the ferromagnetic anion is characterized by peaks around 1.55 and 2.04 eV while the antiferromagnetic state is marked by peaks around 1.55, 1.81, and 2.12 eV, respectively. Combined, these results reproduce correctly, the locations of the three peaks in the experimental spectra. We would, however, like to caution that while such an explanation seems to fit the observed spectra, it does have problems. First, the one electron-levels in the density functional theory do not have a well defined physical meaning. Secondly, adjusting the position of the first peak introduces a fitting procedure that makes the theoretical calculation less than first-principles.

Since the ground states of both neutral and anionic Mn_2O are nearly degenerate, we have examined the possibility that a structural distortion could indeed cause a magnetic transition. We have, therefore, calculated the total energies of the neutral and anionic Mn_2O cluster as a function of the Mn-O-Mn bond angle for the ferro- and antiferromagnetic configuration. For each fixed bond angle, the two Mn-O bonds were optimized. The results for neutral Mn_2O are plotted in Fig. 5. Note that the ferromagnetic configuration is consistently higher in energy than the antiferromagnetic state.

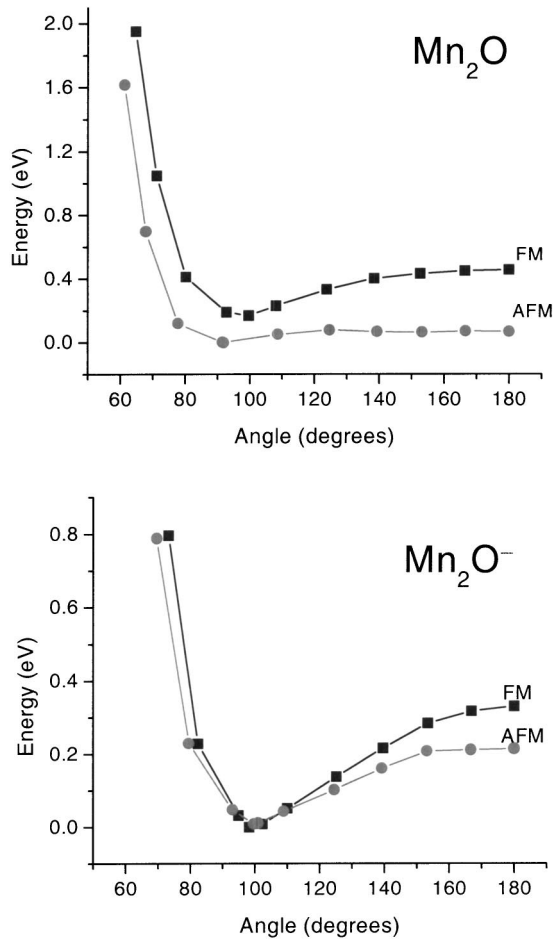


FIG. 5. The energies of neutral and anionic Mn_2O cluster as a function of Mn–O–Mn bond angle for ferromagnetic and antiferromagnetic configurations.

Thus, no structural distortion can lead to a magnetic transition. We will show in the following that the situation is different for the anion.

In Fig. 5 we plot the total energy of the antiferromagnetic and ferromagnetic configuration of Mn_2O^- as a function of Mn–O–Mn bond angle. Once again, for each bond angle, the Mn–O bond lengths were optimized. Note that unlike the case of the neutral cluster, the two curves cross, i.e., there exists a narrow range of angles where the antiferromagnetic state is less stable than the ferromagnetic state. Thus, by structural distortion, it is possible to go from one magnetic state to another. What is even more interesting is that during this transition, the $3d^5$ electrons of each of the Mn atoms are strongly coupled and when spin flip occurs; the spins of all the five electrons flip in unison. This piezomagnetic effect is similar to piezoelectric effect where structural distortion induced by pressure aligns the electric dipole moment. The application of piezoelectric effect in technology is well known. It is thus possible to envision an analogous effect in magnetism where Mn_2O^- embedded in a matrix can be subjected to external pressure and consequently undergo ferro-to antiferromagnetic transition. The question, of course, is whether Mn_2O embedded in a matrix is ferromagnetic. Recall that the neutral Mn_2O is antiferromagnetic.

A system where this transition can be explored is by putting Mn_2O in matrices where there could be a local charge transfer making it locally like an anion and thus stabilizing the ferromagnetic state. One such possibility is doping Mn in metal oxide. Recently, the magnetism of Mn doped ZnO has attracted considerable attention since it has the potential to be ferromagnetic with a room temperature Curie point.¹⁴ In the wurtzite ZnO crystal, the average Zn–O–Zn bond angle is 109° and the average Zn–O distance is 1.98 Å. Note that, in contrast, the Mn–O–Mn bond angle in bulk MnO crystal is 180° and the Mn–O distance is 2.25 Å. It is known from recent experiments¹⁵ that Mn, when doped in ZnO, occupies the Zn site and remains in the Mn^{2+} state. Thus the local geometrical structure of Mn atoms doped in a ZnO matrix is analogous to that of a Mn_2O cluster. Theoretical calculations carried out by Wang *et al.*¹⁶ on a (11–20) slab of Mn doped ZnO predict an antiferromagnetic state which lies 0.21 eV/Mn-atom below the ferromagnetic state. The magnetic moment of Mn is atomiclike, which is consistent with its 2+ valence state. This is what we also find in the neutral and anionic Mn_2O clusters. It will thus be worthwhile to determine, if by distorting the Mn_2O structure in ZnO, the system can be made to undergo a magnetic transition. If so, this will add another functional property to ZnO, which is already known for its electro-optical properties. The almost degenerate ferromagnetic and antiferromagnetic couplings are also likely to lead to interesting temperature dependence of magnetization.

IV. CONCLUSIONS

To conclude, this study shows that the binding energy and magnetic coupling between Mn atoms can be substantially altered by introducing oxygen. A synergistic approach involving accurate first principles theory and photodetachment spectroscopy allowed us to corroborate the nature of magnetic coupling and the magnetic moments with theoretical predictions. The sensitivity of the magnetic coupling to the Mn–O–Mn bond angle in the Mn_2O^- cluster suggests that this may be a prime candidate for exploring piezomagnetic effects at the nanoscale. Independent measurements of the magnetic moment of isolated Mn_2O cluster, both in the gas phase and supported in a matrix, may be very useful to understand the magnetism of nanoscale systems from a fundamental point of view.

ACKNOWLEDGMENTS

The authors are grateful to Professor B. K. Rao for several stimulating discussions. The work at Virginia Commonwealth University was funded in part by a grant from the Department of Energy (DE-FG02-96ER45579). The Johns Hopkins University portion of this work was supported by the Division of Materials Science, Office of Basic Energy Sciences, U.S. Department of Energy under Grant No. DE-FG02-95ER45538. Acknowledgment is also made to the Donors of the Petroleum Research Fund, administered by the American Chemical Society, for partial support of this research (Grant No. 28452-AC6).

- ¹M. D. Morse, Chem. Rev. (Washington, D.C.) **86**, 1049 (1986); R. J. Van Zee, C. A. Baumann, and W. Weltner, Jr., J. Chem. Phys. **74**, 6977 (1981).
- ²A. Arrott, *Magnetism*, edited by G. T. Rao and A. Suhl (Academic, New York, 1966), Vol. 2B, p. 295.
- ³K. D. Bier, T. L. Haslett, A. D. Kirkwood, and M. Moskovits, J. Chem. Phys. **89**, 6 (1988).
- ⁴C. A. Baumann, R. J. Van Zee, S. V. Bhat, and W. Weltner, Jr., J. Chem. Phys. **78**, 190 (1983).
- ⁵S. K. Nayak and P. Jena, Chem. Phys. Lett. **289**, 473 (1998); S. K. Nayak, B. K. Rao, and P. Jena, J. Phys.: Condens. Matter **10**, 10863 (1998); M. R. Pederson, F. Reuse, and S. N. Khanna, Phys. Rev. B **58**, 5632 (1998).
- ⁶M. B. Knickelbein, Phys. Rev. Lett. **86**, 5255 (2001); M. B. Knickelbein, J. Chem. Phys. **116**, 9703 (2002).
- ⁷W. Kohn and L. J. Sham, Phys. Rev. A **140**, 1133 (1965).
- ⁸J. P. Perdew, K. Burke, and M. Ernzerhof, Phys. Rev. Lett. **77**, 3865 (1996).
- ⁹M. R. Pederson and K. A. Jackson, Phys. Rev. B **41**, 7453 (1990).
- ¹⁰K. A. Jackson and M. R. Pederson, Phys. Rev. B **42**, 3276 (1990).
- ¹¹D. V. Porezag and M. R. Pederson, Phys. Rev. A **60**, 2840 (1999).
- ¹²M. Gerhards, O. C. Thomas, J. M. Nilles, W.-J. Zheng, and K. H. Bowen, Jr., J. Chem. Phys. **116**, 10247 (2002).
- ¹³M. Castro, S.-R. Liu, H.-J. Zhai, and L.-S. Wang, J. Chem. Phys. **118**, 2116 (2003).
- ¹⁴T. Dietl, H. Ohno, and F. Matsukura, Phys. Rev. B **63**, 195205 (2001).
- ¹⁵K. V. Rao (private communication).
- ¹⁶Q. Wang, B. K. Rao, and P. Jena (to be published).